Equatorial mixing rates are maximal at the equator rather than minimal.

Reduced mixing from the breaking of internal waves in equatorial waters

Michael C. Gregg, Thomas B. Sanford & David P. Winkel

Applied Physics Laboratory, College of Fishery and Ocean Sciences, University of Washington, Seattle, Washington 98105, USA

In the oceans, heat, salt and nutrients are redistributed much more easily within water masses of uniform density than across surfaces separating waters of different densities. But the magnitude and distribution of mixing across density surfaces are also important for the Earth's climate as well as the concentrations of organisms[1]. Most of this mixing occurs where internal waves break, overturning the density stratification of the ocean and creating patches of turbulence. Predictions of the rate at which internal waves dissipate[2,3] were confirmed earlier at mid-latitudes[4,5]. Here we present observations of temperature and velocity fluctuations in the Pacific and Atlantic oceans between 42° N and 2° S to extend that result to equatorial regions. We find a strong latitude dependence of dissipation in accordance with the predictions[3]. In our observations, dissipation rates and accompanying mixing across density surfaces near the Equator are less than 10% of those at mid-latitudes for a similar background of internal waves. Reduced mixing close to the Equator will have to be taken into account in numerical simulations of ocean dynamics—for example, in climate change experiments.

NO!

Internal waves are generated in the ocean when its stratification is disturbed. Unlike surface waves, which propagate horizontally because they are confined to the air–sea interface, internal waves propagate vertically as well as horizontally, making flow disturbances at the surface or bottom felt in the interior. Garrett and Munk[6] and Munk[7] modelled internal waves in terms of a wavenumber–frequency spectrum; they assumed that the wave field is constant in time, and results from the superposition of many uncorrelated waves having frequencies between the buoyancy frequency N, determined by the stratification, and the Coriolis frequency, $f = 2\Omega_{\mathrm{Earth}} \sin(\theta)$, where Ω_{Earth} is the Earth's rotation rate and θ is the latitude. The Garrett and Munk (GM) frequency spectrum is 'red', with most of the energy very close to f. Integrating components of the GM energy spectrum over the entire range of frequency and wavenumber yields average characteristics of the wave field, such as the net vertical displacement ζ and horizontal wave speed u. Subsequent observations show that the GM model represents the background state of the internal wave field, but some situations are significantly more energetic.

Numerical simulations of energy transfer by interactions within the internal wave field show a net flux towards small spatial scales that increases the shear variance $(\partial u/\partial z)^2$ until it overcomes the stratification and the waves break[2,3]. When the wave field is statistically steady, or varies slowly in time, the rate at which wave breaking dissipates energy approximately equals the rate at which the energy is transferred from large to small scales. This equivalence allows the dissipation rate ε to be expressed in terms of internal wave parameters. To check their numerical simulations, Henyey, Wright and Flatte[3] formulated an analytic model based on the Doppler shifting of evolving test waves by a background wave field. The Doppler shifting produces a net energy flux toward smaller scales—that is, higher wavenumbers—and ultimate breaking. The functional dependence of ε (which is expressed in units of W kg^{-1}) associated with this flux is the product of two terms:

$$\varepsilon = \varepsilon_{30^\circ}\left(N, \Phi_{\mathrm{shear}}(m), \Phi_{\mathrm{strain}}(m)\right) \times L(\theta, N) \qquad (1)$$

The first term, ε at the 30° GM model reference latitude, depends on stratification (via N) and on internal wave characteristics (in terms of spectra of vertical shear, $\Phi_{\mathrm{shear}}(m)$, and of vertical strain, $\Phi_{\mathrm{strain}}(m)$, where m is the vertical wavenumber in cycles per metre). Strain fluctuations are variations of the vertical separations between density surfaces, that is, fluctuations of $\partial\zeta/\partial z$. Previous measurements[4] verified the shear and N dependence in ε_{30°, and subsequent observations[5] and numerical simulations[8] confirmed the strain dependence. The second term contains the latitude (θ) dependence:

$$L(\theta, N) = \frac{f \cosh^{-1}(N/f)}{f_{30^\circ} \cosh^{-1}(N_0/f_{30^\circ})} \qquad (2)$$

Eps/Eps_30

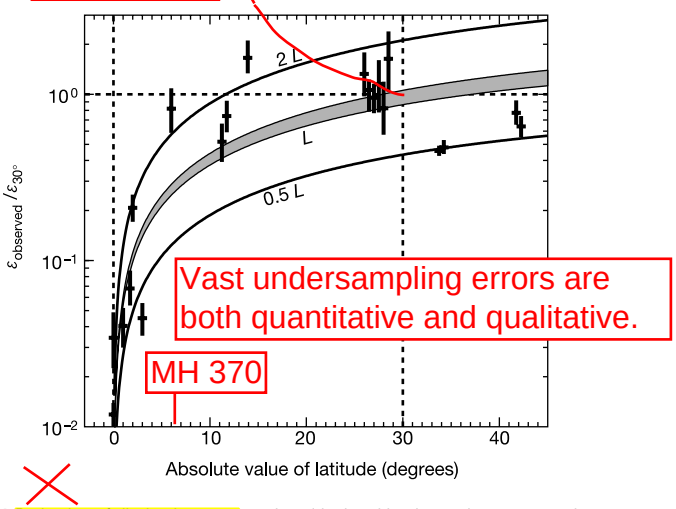

Vast undersampling errors are both quantitative and qualitative.

MH 370

Figure 1 Reduction of dissipation rates produced by breaking internal waves near the Equator. The predicted latitude effect L is unity at 30° because the standard internal wave spectrum, Garrett and Munk[6], and the calculations based on it are referenced to that latitude. Ratios of average $\varepsilon_{\mathrm{observed}}$ to ε_{30° are plotted as short horizontal bars, and upper and lower 95% confidence limits are shown by extents of the vertical lines. Multiple values at the same latitude θ come from different depths or locations. The shaded curve gives the predicted $L(\theta, N)$ for the range of N encountered. Because the N dependence is weak, the height of the shaded band is small. Upper and lower solid lines are twice and one-half the prediction, and approximately bound the scatter in the data. In spite of the scatter, the observations confirm the predicted sharp cut-off of dissipation at low latitude.

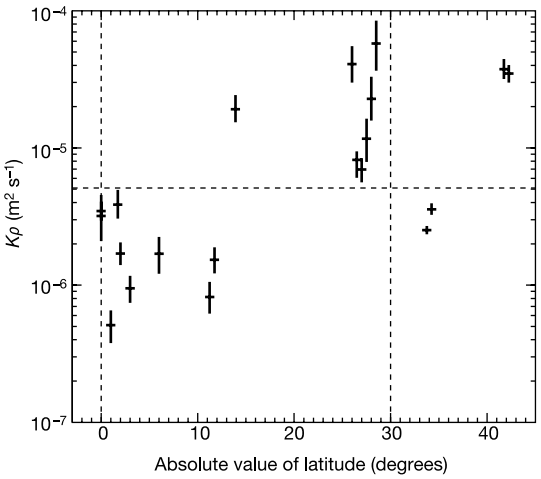

Figure 2 Diapycnal diffusivities. K_ρ was calculated using observed dissipation rates ε and stratification N^2 in equation (2). The horizontal reference line is the value of K_ρ at 30° latitude when internal waves are at the level of the Garrett and Munk spectrum. Owing to the latitude effect on ε produced by internal waves, intense internal waves observed near the Equator produced only modest K_ρ. For reference, the molecular diffusivity of heat in water is 1.4×10^{-7} m^2 s^{-1}.

and is unity at N_0 and 30°. L varies weakly with N, but is independent of internal wave characteristics. The latitude effect arises because the rate at which the evolving waves are Doppler shifted is proportional to the ratio between their vertical and horizontal length scales[9]. This ratio, in turn, depends on their dominant frequency, which is always slightly greater than f and thus varies with latitude.

Our measurements testing L were taken with the Multi-scale Profiler[10] (MSP), a free-fall instrument that resolves velocity and temperature fluctuations from the length of the profile, usually 1,000 m, to centimetre scales of turbulent dissipation. N^2 and strain spectra are obtained from profiles of temperature and salinity. Electromagnetic sensors and an acoustic current meter produce velocity profiles yielding shear with metre-scale resolution. These allow us to evaluate $\varepsilon_{30°}$. The turbulence parameter $\varepsilon_{\text{observed}}$ is obtained independently by measuring centimetre-scale velocity fluctuations with small sensitive probes (airfoils).

In Fig. 1, ratios of $\varepsilon_{\text{observed}}$ to $\varepsilon_{30°}$ are plotted for sets of profiles between the equator and 42° N. Solid curves are L and its multiples. The data scatter by two-fold about L, masking the latitude effect at mid-latitudes[4], but not at low latitudes, where dissipation rates are sharply cut off. Near and on the Equator, $\varepsilon_{\text{observed}}$ is only 1–6% of mid-latitude ratios, confirming the prediction.

Most numerical models express diapycnal mixing in terms of an eddy coefficient K_ρ. When the average dissipation rate nearly balances the rate at which breaking internal waves produce turbulence, the mixing can be estimated simply[11] as:

$$K_\rho \approx 0.2\varepsilon/N^2 \tag{3}$$

where K_ρ is in units of $m^2\,s$. Application of this local estimate to the large-scale mean circulation is *ad hoc*[12], but comparisons of observations like ours with the rate of thickening of tracer clouds injected into the thermocline[13] and into abyssal[14,15] waters confirm the estimates. For our observations, K_ρ is markedly smaller at low latitudes than at mid-latitudes (Fig. 2). The smallest values are only a few times larger than the molecular diffusivity of heat in these waters, $1.4 \times 10^{-7}\,m^2\,s^{-1}$, demonstrating that at some times and places diapycnal mixing is negligible in the equatorial ocean.

To appreciate fully the effect of the low-latitude cut-off of internal wave mixing, it is necessary to examine the intensity of the internal wave field. The most important term in $\varepsilon_{30°}$ is the square of the ratio of the observed shear spectrum to the shear variance predicted by the GM model: this term varies from 0.32 to 1,140 (Fig. 3). In view of such a large range, the two-fold scatter in the scaled dissipation rates is rather small. The three largest spectral ratios are on and close to the Equator. Were it not for the sharp latitudinal cut-off near the Equator, this trio would have produced the largest K_ρ in our data.

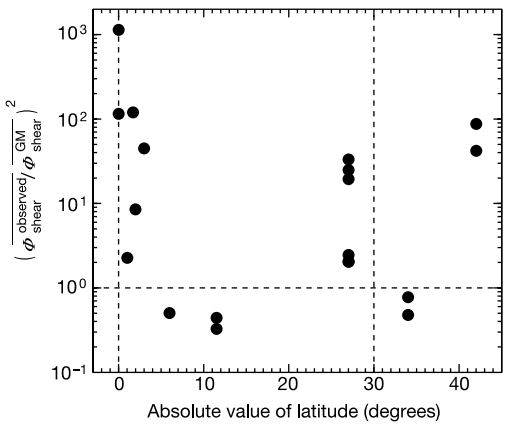

Figure 3 Effect of internal wave intensity on dissipation. The most important scaling term in equation (4) is $(0.1/k_c)^2$ which is plotted here in its more physical form as $\left(\overline{\Phi}^{\text{observed}}_{\text{shear}} / \overline{\Phi}^{\text{GM}}_{\text{shear}}\right)^2$. The horizontal dotted line at unity is the level for the GM model internal wave spectrum at 30° latitude. Some of the low-latitude measurements reveal very intense internal waves close to and on the Equator.

Table 1 **Multi-scale profile**

Latitude	Longitude	Expedition	Refs	Profiles
0°	156° E	COARE3	19	34
0°	140° W	Tropic Heat 2	20	69
1° N	140° W	Tropic Heat 2	20	7
1.7° S	156° E	COARE3	19	28
2° N	140° W	Tropic Heat 2	20	5
3° N	156° E	COARE3	19	12
6° N	140° W	Tropic Heat 2	20	3
11.5° N	134.8° W	Tropic Heat 2	20	5
13.9° N	59° W	C-SALT edge	21, 22	4
27° N	79.4° W	Florida Straits stn 5&6	23	10
34° N	127° W	PATCHEX	4, 24	27
42° N	126° W	PATCHEX north	4	5

Locations, expedition names with citations of relevant publications, and number of profiles of the data used in this comparison.

The agreement between observations and theory at low latitudes is better than expected (F. Henyey, personal communication), because it is unlikely that the GM model should be accurate close to the Equator and linear approximations made to obtain the dissipation model may not hold. For instance, the shear/strain correction accounts for only one of the ways in which a wave field can depart from the GM model, and more radical departures may occur where f is very small. We, therefore, interpret Fig. 1 as confirmation that the wave–wave interactions leading to ultimate breaking, energy dissipation, and diapycnal mixing do indeed vary with latitude, and that the effect is most important at low latitudes. The result is sufficiently robust to be used in numerical models, but internal wave measurements that are more detailed and of longer duration than ours are needed before we can be confident that we fully understand the mechanisms involved. For example, small but finite dissipation rates were observed on the Equator where no dissipation is predicted. They may indicate the importance of nonlinearities not considered in the prediction, but they could also result from either small mean shears enhancing mixing above the levels produced solely by internal wave interactions, or from effects of horizontal changes in mean currents, which are also neglected in the prediction.

Because mixing matters in the ocean, it must be represented accurately in models. Mapping dissipation rates throughout the ocean is a daunting task that is made considerably easier if mixing can be estimated from internal wave parameters, stratification and latitude; internal wave fields appear to be horizontally coherent over much larger scales than mixing patches, and to vary more slowly. Consequently, if the production of mixing by internal waves is understood and quantified, the problem of mapping mixing can be transferred to larger spatial scales and slower timescales by mapping internal waves. This requires a large effort, but the task is feasible. The result, however, would not be adequate for predicting mixing in future oceans having altered stratification and forced by differing wind patterns. Developing realistic climate prediction also requires understanding of how internal waves are generated, so the global field can be modelled realistically. For example, the only mixing measurements repeated at the same place during different seasons showed hints of a seasonal dependence[16], and numerical modelling is now showing how internal waves may vary in response to seasonal changes in wind stress[17]. A first attempt at a comprehensive model is under way (P. Muller, personal communication, 2002), but many more observations of internal waves and mixing will be needed to verify its predictions. The observations presented here confirm part of the input needed for comprehensive understanding and global modelling of internal waves and mixing. □

Methods

MSP data

Table 1 gives the positions and number of MSP profiles forming the station averages, and references to the expeditions that collected them. We used data from below the seasonal thermocline, where the GM model should apply, and where the mean shear was weak. Owing to the strong mean shear in the main thermocline near and on the Equator during Tropic Heat 2, only data from the lower thermocline were used. COARE3 data on the Equator were used between 400–640 m and 640–890 m because we found no significant mean shear. Mean shear was weak near the centre of the Straits of Florida at stations 5 and 6, which were averaged between 205–305, 305–405 and 405–505 m. The C-SALT profiles were taken just outside the thermohaline staircase.

Dissipation rates

Shear spectra of airfoil records were calculated over 2-m intervals, and integrated to estimate local dissipation rates along each profile. Histograms of each depth interval and station were examined to estimate the noise level for the ensemble. The noise levels varied from 5×10^{-11} to 8×10^{-11} W kg^{-1}, probably owing to differing noise characteristics of the airfoils. Estimates at or below the noise level were set to zero on the assumption that no mixing occurred. This was consistent with the lack of identifiable density overturns in these intervals, but we could not always be certain owing to the half-metre vertical resolution attainable with the Sea-Bird temperature and salinity records. Averages and confidence limits were computed using bootstrap[18] techniques. Zeroing noisy ε values made little difference in most averages, but it reduced the COARE3 deep average at 3° N by one-half, and the Tropic Heat 2 data at 11.5° N by two-thirds. Using the unconditional averages would put the former within and the latter above the plotted bounds of 0.5 and 2 times the prediction.

Predicting the dissipation rate

Dissipation rates were predicted by evaluating the first part of equation (1) expressed as:

$$\varepsilon_{30^\circ} = 6.73\times10^{-10}\left(\frac{N}{N_0}\right)^2\left(\frac{0.1}{k_c}\right)^2\left(\frac{1+1/R}{4/3}\right)\left(\frac{2}{R-1}\right)^{1/2} \quad (4)$$

where ε_{30° is in units of W kg^{-1}. This equation of is a slight modification of the formulation of ref. 5. N_0 is the GM model reference stratification 5.24×10^{-3} s^{-1}, k_c is the high-wavenumber cut-off of the internal wave shear spectrum, and R is a dimensionless ratio defined below. To accommodate varied spectral shapes, the shear spectrum is integrated until the variance reaches $0.661\,N^2$, that is, $\int_{k_0}^{k_c}\Phi_{\text{shear}}^{\text{observed}}(m)\,dm = 0.661N^2$. The upper limit k_c is taken to be the high-wavenumber cut-off, and k_0 is the reciprocal of the length of record being analysed. The reference variance is obtained by integrating the white GM shear spectrum to its cut-off at 0.1 cycles per metre, that is $\int_{0.005}^{0.1}\Phi_{\text{shear}}^{\text{GM}}(m)\,dm = 0.661N^2$. Consequently, at vertical wavenumbers less than k_c, the ratio of the average spectral levels is $\Phi_{\text{shear}}^{\text{observed}}/\Phi_{\text{shear}}^{GM} = 0.1/k_c$. The second term in equation (4) is the square of this ratio, and is plotted in Fig. 3. R is the average ratio of the shear variance normalized by N^2 to the strain variance, both integrated to k_c. Dependent on R, the third and fourth terms in equation (4) are corrections for variations in the ratio of total energy to horizontal kinetic energy and in the dominant frequency content, both relative to the GM model.

The latitude dependence, equation (2), is the analytic form in the theoretical model[3] and has not been previously tested. As noted earlier, it arises because the rate at which the evolving waves are Doppler shifted depends on the ratio between their vertical and horizontal length scales. This is expressed by $\frac{l_{\text{vert}}}{l_{\text{horiz}}} = \left\langle\frac{\omega^2-f^2}{N^2-\omega^2}\right\rangle_{\text{GM}}^{1/2} = \frac{f}{N}\cosh^{-1}\left(\frac{N}{f}\right)$, where averaging is across the internal wave frequency range, $f \leqq \omega \leqq N$, and is weighted by the frequency content of the GM wave field. Comparison to the GM reference at 30° leads to equation (2). Because N/f is a large number, $\cosh^{-1}(N/f) \approx \ln(2N/f)$.

Received 19 July 2002; accepted 14 February 2003; doi:10.1038/nature01507.

1. National Science Foundation *Ocean Sciences at the New Millennium* (NSF, Washington DC, 2001).
2. McComas, C. H. & Muller, P. The dynamic balance of internal waves. *J. Phys. Oceanogr.* **11,** 970–986 (1981).
3. Henyey, F. S., Wright, J. & Flatte, S. M. Energy and action flow through the internal wave field: An eikonal approach. *J. Geophys. Res.* **91,** 8487–8495 (1986).
4. Gregg, M. C. Scaling turbulent dissipation in the thermocline. *J. Geophys. Res.* **94,** 9686–9698 (1989).
5. Polzin, K., Toole, J. M. & Schmitt, R. W. Finescale parameterization of turbulent dissipation. *J. Phys. Oceanogr.* **25,** 306–328 (1995).
6. Garrett, C. J. R. & Munk, W. H. Space-time scales of internal waves: A progress report. *J. Geophys. Res.* **80,** 291–297 (1975).
7. Munk, W. H. in *Evolution of Physical Oceanography* (eds Warren, B. A. & Wunsch, C.) 264–291 (MIT Press, Cambridge, Massachusetts, 1981).
8. Sun, H. & Kunze, E. Internal wave-wave interactions. Part II: Spectral energy transfer and turbulence production. *J. Phys. Oceanogr.* **29,** 2905–2919 (1999).
9. Henyey, H. F. in *Dynamics of Internal Gravity Waves in the Ocean: Proceedings,'Aha Huliko'a Hawaiian Winter Workshop* (eds Muller, P. & Henderson, D.) 233–236 (Spec. publ. SOEST, Univ. Hawaii, 1991).
10. Winkel, D. P., Gregg, M. C. & Sanford, T. B. Resolving oceanic shear and velocity with the Multi-Scale Profiler. *J. Atmos. Ocean. Technol.* **13,** 1046–1072 (1996).
11. Osborn, T. R. Estimates of the local rate of vertical diffusion from dissipation measurements. *J. Phys. Oceanogr.* **20,** 83–89 (1980).
12. Davis, R. E. Diapycnal mixing in the ocean: The Osborn-Cox model. *J. Phys. Oceanogr.* **24,** 2560–2576 (1994).
13. Ledwell, J. R., Watson, A. J. & Law, C. S. Evidence for slow mixing across the pycnocline from an open-ocean tracer release experiment. *Nature* **364,** 701–703 (1993).
14. Toole, J. M., Polzin, K. L. & Schmitt, R. W. Estimates of diapycnal mixing in the abyssal ocean. *Science* **264,** 1120–1123 (1994).
15. Ledwell, J. R. *et al.* Evidence for enhanced mixing over rough topography in the abyssal ocean. *Nature* **403,** 179–182 (2000).
16. Gregg, M. C. Variations in the intensity of small-scale mixing in the main thermocline. *J. Phys. Oceanogr.* **7,** 436–454 (1977).
17. Nagasawa, M., Niwa, Y. & Hibiya, T. Spatial and temporal distribution of wind-induced internal wave energy available for deep water mixing in the North Pacific. *J. Geophys. Res.* **105,** 13933–13943 (2000).
18. Efron, G. & Gong, G. A leisurely look at the bootstrap, the jackknife, and cross-validation. *Am. Stat.* **37,** 36–48 (1983).
19. Gregg, M. C., Winkel, D. P., Sanford, T. B. & Peters, H. Turbulence produced by internal waves in the oceanic thermocline at mid and low latitudes. *Dynam. Atmos. Oceans* **24,** 1–14 (1996).
20. Peters, H., Gregg, M. C. & Sanford, T. B. Equatorial and off-equatorial shear variability at 140° W. *J. Geophys. Res.* **96,** 16913–16928 (1991).
21. Schmitt, R. W., Perkins, H., Boyd, J. D. & Stalcup, M. C. C-SALT: an investigation of the thermohaline staircase in the western tropical North Atlantic. *Deep-Sea Res.* **34,** 1655–1665 (1987).
22. Gregg, M. C. & Sanford, T. B. Shear and turbulence in thermohaline staircases. *Deep-Sea Res.* **34,** 1689–1696 (1987).
23. Winkel, D. P., Gregg, M. C. & Sanford, T. B. Patterns of shear and turbulence across the Florida Current. *J. Phys. Oceanogr.* **32,** 3269–3285 (2002).
24. Gregg, M. C. & Sanford, T. B. The dependence of turbulent dissipation on stratification in a diffusively stable thermocline. *J. Geophys. Res.* **93,** 12381–12392 (1988).

Acknowledgements The Office of Naval Research and the National Science Foundation funded our instrumentation and data collection. A SECNAV/CNO fellowship in oceanography supported M.C.G. during the analysis and writing of this letter.

Competing interests statement The authors declare that they have no competing financial interests.

Correspondence and requests for materials should be addressed to M.C.G. (e-mail: gregg@apl.washington.edu).

This Gregg et al. paper is highly misleading. Vast undersampling errors of turbulence and turbulent mixing occur at the equator because Coriolis forces vanish. From the Kolmogorov intermittency law, dissipation rates are lognormal. Intermittency factors are maximal, as described by Baker and Gibson (1987), explaining the catastrophic equatorial icing phenomenon discussed in Volumes 21-25 of the Journal of cosmology. See for example: http://JournalofCosmology.com/JOC24/AGU2014.pdf .

Turbulence is now a solved problem, rather than a mystery of classical physics. Many mysteries can now be explained, starting with the hot big bang itself at Planck scales where energy is extracted from the vacuum by turbulent combustion at 10^32 K, and preserved by cosmic microwave background fossils. Eleven decades of the great power law on the sky support universal Kolmogrovian similarity laws.

"Turbulence measurements at the Equator are vastly undersampled." Commentary on "Reduced mixing from the breaking of internal waves in equatorial waters", Gregg et al., Nature (2003), Carl H. Gibson, Vol. 25, No. 38, pp 13667-13670.